Journal of Rock Mechanics and Geotechnical Engineering 12 (2020) 682–692

Contents lists available at ScienceDirect

Journal of Rock Mechanics and Geotechnical Engineering

journal homepage: www.jrmge.cn

Full Length Article

Effective thermal conductivity of an intact heterogeneous limestone

A.P.S. Selvadurai [a,*], S.M. Rezaei Niya [b]

[a] Department of Civil Engineering and Applied Mechanics, McGill University, Montréal, QC, H3A 0C3, Canada
[b] Royal Melbourne Institute of Technology, Melbourne, Australia

ARTICLE INFO

Article history:
Received 5 December 2019
Received in revised form
17 March 2020
Accepted 12 April 2020
Available online 8 May 2020

Keywords:
Thermal conductivity
Cobourg limestone
Multi-phasic approach
Voigt, Reuss and Hill estimates
Hashin and Shtrikman bounds
Computational modeling

ABSTRACT

The Cobourg limestone is a very low porosity rock consisting of lighter nodular regions that are predominantly calcite and darker regions consisting of calcite, quartz, dolomite, and an appreciable clay fraction. This paper presents the application of the theory of multi-phasic composites to estimate the possible maximum effective thermal conductivity of the heterogeneous rocks. The thermal conductivity estimates are expected to be representative of the intact rock, without fractures or fissures that can influence the heat conduction process. The estimates are therefore indicative of the thermal properties of the rock in undisturbed regions unaffected by the influences of stress relief and excavation damage during construction of deep ground repositories for the disposal of heat-emitting nuclear waste.

1. Introduction

The estimation of thermal properties of materials is one of the most widely investigated topics in the engineering sciences. Since the development of Fourier's theory of heat conduction (Fourier, 1822), the thermal properties of materials relevant to problems in engineering, physics and earth sciences have been extensively investigated. These studies deal with a variety of topics including (i) the basic thermal conductivity properties of crystals, (ii) thermal conductivity of multi-phasic composites and crystalline solids, (iii) influence of temperature and mass transfer on thermal conductivity, (iv) phase transformation during heating, (v) electrochemical and pore space topology alterations during heat conduction, (vi) development of laboratory-based experimental techniques for measurement of thermal properties, and (vii) field studies of thermal conductivity at the regional and continental scales. Clearly, the presentation of an all-encompassing review of heat-conduction, even restricted to geologic media, is a daunting task and certainly beyond the scope of this article.

Some noteworthy references related to this topic include the pioneering studies by Birch and Clark (1940a, b), Horai and Simmons (1969), Horai (1971), Kappelmeyer and Haenel (1974), Cermak and Rybach (1982), Robertson (1988), Brigaud and Vasseur (1989), Vasseur et al. (1995) and the recent article by Merriman et al. (2018) that specifically deals with the thermal conductivity of carbonate minerals and rocks. These articles themselves contain extensive references related to thermal conductivity properties of geologic media.

The deep geological disposal of nuclear waste in competent rock formations is being considered by many countries including Canada, Finland, France, Sweden, Switzerland, etc. (Côme et al., 1985; Laughton et al., 1986; Chapman and McKinley, 1987; OECD, 1988; Gnirk, 1993; Gray, 1993; Selvadurai and Nguyen, 1996; Selvadurai, 1997, 2017; IAEA, 2000; NIREX, 2004; Rutqvist et al., 2004, 2005; Alonso et al., 2005; Brady et al., 2009; Pusch et al., 2011; Selvadurai et al., 2011, 2015; NWMO, 2011a, b; Selvadurai and Jenner, 2013; OPG, 2016; Selvadurai and Najari, 2016, 2017; Yardley et al., 2016; Selvadurai and Glowacki, 2017, 2018). A recent review of international research efforts related to deep geological disposal of heat-emitting high-level nuclear fuel waste has also been compiled by Faybishenko et al. (2016).

This study examines an aspect of the potential of the Cobourg limestone for siting a deep ground repository (DGR) for high-level nuclear waste in the Cobourg formation (argillaceous limestone). In Canada, the heterogeneous Cobourg limestone (Fig. 1) and the surrounding geologic media were identified as a potential host rock for constructing a DGR to store low- and intermediate-level *non-heat emitting* radioactive waste. A description of the geological

* Corresponding author.
E-mail address: patrick.selvadurai@mcgill.ca (A.P.S. Selvadurai).
Peer review under responsibility of Institute of Rock and Soil Mechanics, Chinese Academy of Sciences.

https://doi.org/10.1016/j.jrmge.2020.04.001

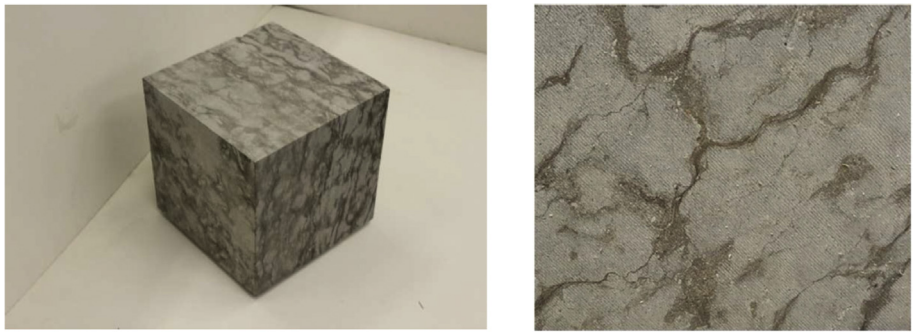

(a) (b)

Fig. 1. The Cobourg limestone: (a) The heterogeneous features; and (b) The arrangement of the facies over a 100 mm × 120 mm area (Selvadurai, 2019a, b).

setting of the rock formations containing the Cobourg limestone was given in NWMO (2011b).

The investigation of the thermal properties of the Cobourg limestone, as a reference sedimentary rock from southern Ontario, Canada, was undertaken to supplement the research base necessary for understanding the suitability of sedimentary geologic formations for storage of high-level nuclear fuel waste. This high-level waste is currently stored at the reactor sites and contributes to a growing environmental risk as the reactors age and approach their reliable life span. In the development of models to describe the coupled thermo-hydro-mechanical behavior of repository rocks (e.g. Selvadurai and Nguyen, 1995; Stephansson et al., 1996; Selvadurai and Suvorov, 2016), the experimental evaluations of the parameters governing the coupled processes should address the issue of the representative volume element (RVE) needed to obtain meaningful effective properties of the heterogeneous Cobourg rock. Bulk mass density and uniaxial compressive strength measurements point to size-dependency effects (Selvadurai, 2017, 2019a) and suggest that sample sizes with dimensions greater than 75 mm will provide a suitable RVE to estimate the intact geomechanical properties. Large sample dimensions are needed to adequately capture the heterogeneity, but this carries with it the development of experimental facilities and methodologies that are non-routine. For example, the estimation of the poroelastic Biot coefficient (Biot, 1941) of the Cobourg limestone was discussed by Selvadurai (2019a). The extremely low permeability of the Cobourg limestone (i.e. permeability K in the range of 10^{-23}-10^{-19} m^2 from Vilks and Miller (2007) and Selvadurai (2019b)) means that an inordinate amount of time is required to saturate the rock and for the pressures applied at the boundary of the sample to reach and equalize at its interior. This is essential to accurately determine the elastic compressibility of the solid material composing the rock. To avoid this drawback, Selvadurai (2019a) used multi-phasic approaches to determine the solid material compressibility, providing a convenient method to estimate the Biot coefficient for very low permeability rocks. Selvadurai et al. (2019) used a similar approach to estimate the Biot coefficient of Grimsel granite. Selvadurai (2019b) showed that the multi-phasic approach can be used to estimate the effective permeability of a heterogeneous rock. The purpose of the present study is to apply the multi-phasic approach to estimate the effective thermal conductivity of the Cobourg limestone. The methodology follows from approaches adopted to estimate the thermal conductivity of rocks and other composites (Budiansky, 1970; Horai, 1971; Christensen, 1979; Brigaud and Vasseur, 1989; Pribnow and Umsonst, 1993; Vasseur et al., 1995; Revil, 2000).

2. The Cobourg mineralogy

The mineralogical compositions of the lighter and darker facies of the Cobourg limestone were obtained by Waber et al. (2007) (see also Koroleva et al., 2009) using the RIETVELD approach. The results obtained by Waber et al. (2007) are shown in Table 1. The mineralogical compositions were also obtained using the X-ray diffraction (XRD) facilities available in the McGill Institute for Advanced Materials (MIAM). A disc specimen measuring approximately 140 mm in diameter and 5 mm in thickness was used to obtain samples of the two regions of the limestone; other samples were also obtained without any preference for the facies that were present. The tests were performed using the Bruker D8 Discovery X-ray diffractometer and the mineralogical compositions were determined using the DIFFRAC.EVA software. The results are shown in Table 2 for comparison purposes. The estimations of the clay fractions in particular require experience in sample preparation and the interpretation of the XRD data. In this regard, the RIETVELD approach is expected to give better estimates of the clay fraction.

In consideration of the relative merits of the XRD interpretation approaches, we used the data obtained by Waber et al. (2007) for the mineralogical compositions of the lighter and darker facies (Table 1). Other features of the rock are given by Selvadurai (2017, 2019a, b). The relative proportions of the lighter and darker facies were also estimated by dissecting an 80 mm × 100 mm × 300 mm cuboidal sample of the Cobourg limestone into 10 adjacent thick slabs measuring 80 mm × 100 mm × 8 mm. Photographic imaging of the larger surfaces of the slabs and their assembly was used to reconstruct the interior distribution of the lighter and darker facies. Details of the procedures used were fully documented by Selvadurai (2017). The reconstructed image of the plausible distribution of the lighter and darker species of the Cobourg limestone is shown in Fig. 2. The digitized images of the larger surface of the slabs were also used to reconstruct the interior distribution of the facies of the limestone. Both extrusion from the large surfaces and a solid modeling technique were used to reconstruct the species

Table 1
Mineralogical compositions of the lighter and darker facies of the Cobourg limestone. Data were obtained by Waber et al. (2007) and interpreted using the RIETVELD approach. It should be noted that (i) Smaller fractions of albite, K-feldspar and pyrites have been grouped with quartz; (ii) Small fractions of siderite were grouped with dolomite; and (iii) Chlorite is grouped with kaolinite.

Cobourg limestone	Mineralogical composition (%)					
	Calcite	Quartz	Dolomite	Illite	Kaolinite	Montmorillonite
Lighter facies	80	5	3	7	4	1
Darker facies	63	11	5	14	4	3

Table 2
Mineralogical compositions of the Cobourg limestone and its lighter and darker facies. Data were obtained from the McGill Institute for Advanced Materials (MIAM). XRD data were interpreted using the DIFFRAC.EVA software.

Material	Mineralogical composition (%)					
	Calcite	Quartz	Dolomite	Illite	Kaolinite	Montmorillonite
Cobourg limestone	76.4	11.5	3	0.9	2.8	5.3
Lighter facies	82.4	7.5	1.3	0.8	2.2	5.8
Darker facies	69.5	16.9	4.2	1.2	2.9	5.3

arrangements within the thick slab. The details of the procedures were documented in Selvadurai (2019b).

The volume fractions of the separate regions were estimated in previous research efforts (Selvadurai, 2017, 2019a, b); the average volume fraction of the darker species is estimated (Fig. 2) to be $V_{DR} \simeq 0.54$. There can be a wide variability in estimation of the relative volume fractions, with estimates as low as $V_{DR} \simeq 0.35$ (Selvadurai, 2017, 2019a, b). For the purposes of illustrating the application of a multi-phasic approach to estimate the thermal conductivity, we selected the following volume proportions: $V_{DR} \simeq 0.54$ and $V_{LR} \simeq 0.46$, where V_{LR} is the volume fraction of the lighter facies.

3. Multi-phasic estimates of thermal conductivity

The two facies of the rock are composed of the basic minerals calcite, dolomite, quartz, clay and voids in varying proportions. To apply the multi-phasic approach, we required the thermal properties of these basic minerals. Extensive studies have been conducted by various investigators to estimate the thermal conductivities of what are largely crystals, with thermal conductivities that are anisotropic, i.e. the thermal conductivity is a second-order tensor with three principal values. For the minerals identified, the thermal conductivity is either isotropic, with a single thermal conductivity, or transversely isotropic such that the thermal conductivities can be identified either along or normal to the crystal planes. In order to assign a specific estimate for the effective thermal conductivity, the measure adopted is the geometric mean, given by

$$k_{GM} = \sqrt[3]{k_t^2 k_n} \tag{1}$$

where k_t is the thermal conductivity along the planes of stratification and k_n is the thermal conductivity normal to the planes of stratification. The geometric mean concept was used by Pribnow and Umsonst (1993) to estimate the thermal conductivity of quartzitic rocks (their estimate for $k_{GM} = \sqrt{k_t k_n}$, as opposed to Eq. (1)) and in estimation of the fluid transport characteristics of heterogeneous porous media (Selvadurai and Selvadurai, 2010, 2014), where the permeabilities are non-zero and are roughly of the same order of magnitude in each of the three orthogonal directions. The estimation of the thermal conductivity of the minerals listed previously presents a challenge, since there is variability in the estimates given in the literature. The thermal conductivities also exhibit a temperature dependency, with a reduction in the thermal conductivities as the temperature increases. For consistency, we selected the data provided by Robertson (1988), who used estimates provided by Birch and Clarke (1940a, b) and the estimates given by Brigaud and Vasseur (1989) and Vasseur et al. (1995) (see Table 3).

4. Effective thermal conductivity of the Cobourg limestone

Assuming that the Cobourg limestone can be modeled as a medium where the facies are spatially distributed, which leads to a medium with isotropic effective properties, and provided that the phasic thermal conductivities do not lead to non-conducting thermal barriers, the effective thermal conductivity (k^*) can be bounded by the *upper bound* Voigt (1928) and the *lower bound* Reuss (1929) estimates in the form of (see also Wiener, 1912):

$$\left[\sum_{i=1}^{m}\left(\frac{V_i}{k_i}\right)\right]^{-1} < k^* < \sum_{i=1}^{m}(k_i V_i) \tag{2}$$

where subscript i represents the calcite, dolomite, quartz, Montmorillonite and kaolinite; V_i is the volume fraction indicated in Table 2; and k_i is the respective thermal conductivity of the phase indicated in Table 3.

4.1. Thermal conductivity of the Cobourg limestone at 273 K

Considering volume fractions given in Table 2 and the thermal conductivity estimates for constituent minerals given in Table 3, and applicable to 273 K, the Voigt (1928) and Reuss (1929) bounds

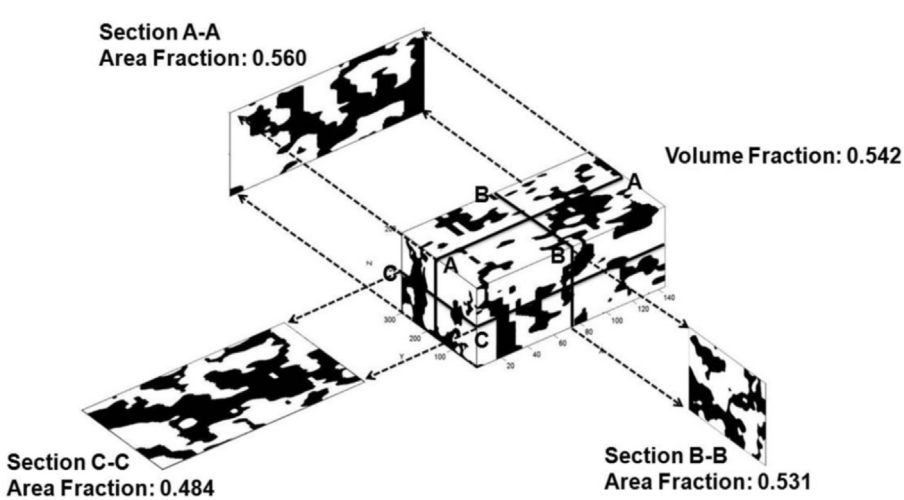

Fig. 2. The lighter and darker facies within the Cobourg limestone (after Selvadurai, 2019b). Area fraction = A_{DR}/A, and volume fraction = V_{DR}/V, where A_{DR} and V_{DR} refer to the area and volume fractions of the darker facies, respectively; and A and V refer to the total area and total volume, respectively.

Table 3
Thermal conductivity of the basic minerals in the Cobourg limestone. The values for the clay minerals correspond to those applicable to their dry states.

Mineral	Source	Thermal conductivity (W/(m K))	
		$T = 273$ K	$T = 373$ K
Calcite	Robertson (1988)	4 (parall.) 3.5 (perp.) 3.83 (effective)	3.05 (parall.) 2.75 (perp.) 2.95 (effective)
Quartz	Robertson (1988)	12 (parall.) 6.8 (perp.) 9.93 (effective)	8 (parall.) 5 (perp.) 6.84 (effective)
Dolomite	Robertson (1988)	5.6	5.4
Illite	Brigaud and Vasseur (1989); Vasseur et al. (1995)	1.8	1.6
Kaolinite	Brigaud and Vasseur (1989); Vasseur et al. (1995)	2.6	1.8
Montmorillonite	Brigaud and Vasseur (1989); Vasseur et al. (1995)	2	1.7

Note: T denote the temperature; parall. refers to the direction along the laminations or planes of transverse isotropy or orthotropy; and perp. refers to the direction perpendicular to the planes of transverse isotropy or orthotropy.

(Eq. (2)) give the following range for the thermal conductivity of the lighter and darker facies in the Cobourg limestone:

$$3.59\ \mathrm{W/(m\ K)} < k^*_{273\ \mathrm{K}} < 3.98\ \mathrm{W/(m\ K)} \quad \text{(lighter)} \tag{3}$$

$$3.42\ \mathrm{W/(m\ K)} < k^*_{273\ \mathrm{K}} < 4.2\ \mathrm{W/(m\ K)} \quad \text{(darker)} \tag{4}$$

Considering these results, the Voigt (1928) and Reuss (1929) bounds can be combined to provide the Hill (1952) estimates, i.e.

$$\left(k^*_{273\ \mathrm{K}}\right)_{\mathrm{LR}} = 3.78\ \mathrm{W/(m\ K)};\ \left(k^*_{273\ \mathrm{K}}\right)_{\mathrm{DR}} = 3.81\ \mathrm{W/(m\ K)} \tag{5}$$

An improvement to the Hill (1952) average based on the Voigt (1928) and Reuss (1929) bounds can be obtained using the results given by Hashin and Shtrikman (1962) for a two-phase system. In this instance, the two constituents can be identified as the two separate facies with $V_{\mathrm{DR}} \simeq 0.54$ and $V_{\mathrm{LR}} \simeq 0.46$; this is an appropriate assumption that is consistent with the very low porosity of the lighter ($n_{\mathrm{LR}} \simeq 0.006$) and darker ($n_{\mathrm{DR}} \simeq 0.01$) facies.

Using the Hashin and Shtrikman (1962) bounds for the bulk thermal conductivity of the heterogeneous limestone, consisting of the lighter and the darker facies in the volume fractions indicated previously, we obtain

$$\left(k^*_{273\ \mathrm{K}}\right)_{\mathrm{LR}} + \frac{V_{\mathrm{DR}}}{\frac{1}{\left(k^*_{273\ \mathrm{K}}\right)_{\mathrm{DR}} - \left(k^*_{273\ \mathrm{K}}\right)_{\mathrm{LR}}} + \frac{V_{\mathrm{LR}}}{3\left(k^*_{273\ \mathrm{K}}\right)_{\mathrm{LR}}}} \le k^*_{273\ \mathrm{K}} \le \left(k^*_{273\ \mathrm{K}}\right)_{\mathrm{DR}} + \frac{V_{\mathrm{LR}}}{\frac{1}{\left(k^*_{273\ \mathrm{K}}\right)_{\mathrm{LR}} - \left(k^*_{273\ \mathrm{K}}\right)_{\mathrm{DR}}} + \frac{V_{\mathrm{DR}}}{3\left(k^*_{273\ \mathrm{K}}\right)_{\mathrm{DR}}}} \tag{6}$$

This result gives

$$3.7961803\ \mathrm{W/(m\ K)} < k^*_{273\ \mathrm{K}} < 3.7961804\ \mathrm{W/(m\ K)} \tag{7}$$

The bounds give identical results and, in view of the near equal volume fractions V_{DR} and V_{LR}, are close to the average thermal conductivity of the lighter and darker phases given by Eq. (5).

4.2. Thermal conductivity of the cobourg limestone at 373 K

The procedure can be extended to estimate the effective thermal conductivity of the Cobourg limestone at other temperatures. Considering the thermal conductivity estimates for the constituent minerals given in Table 3, and applicable to 373 K, the Voigt (1928) and Reuss (1929) bounds for the thermal conductivities of the lighter and darker facies are given by

$$2.81\ \mathrm{W/(m\ K)} < k^*_{373\ \mathrm{K}} < 3.06\ \mathrm{W/(m\ K)} \quad \text{(lighter)} \tag{8}$$

$$2.73\ \mathrm{W/(m\ K)} < k^*_{373\ \mathrm{K}} < 3.23\ \mathrm{W/(m\ K)} \quad \text{(darker)} \tag{9}$$

The corresponding Hill (1952) estimates are

$$\left(k^*_{373\ \mathrm{K}}\right)_{\mathrm{LR}} = 2.94\ \mathrm{W/(m\ K)};\ \left(k^*_{373\ \mathrm{K}}\right)_{\mathrm{DR}} = 2.98\ \mathrm{W/(m\ K)} \tag{10}$$

The Hashin and Shtrikman (1962) results give the following bounds:

$$2.961555\ \mathrm{W/(m\ K)} < k^*_{373\ \mathrm{K}} < 2.9615554\ \mathrm{W/(m\ K)} \tag{11}$$

Again, the bounds coincide and, considering the near equal proportions of the lighter and darker fractions, the results are close to the Hill (1952) averages, indicated by Eq. (10).

5. A fabric-based thermal conductivity estimation of the Cobourg limestone

Ideally, the mapping of the internal fabric of the limestone that contributes to the heterogeneity should be performed using non-invasive techniques such as X-ray tomography (XRT) imaging. This procedure was attempted on the smaller cylindrical samples but the sample dimensions could not provide accurate mapping of an RVE. As an alternative, a cuboidal block (80 mm × 100 mm × 300 mm) of the rock was dissected to recover 10 thick adjacent slabs measuring 80 mm × 100 mm × 8 mm. Both surfaces of each slab were photographed and digitally imaged, and a MATLAB software-based image processing technique was used to create black and white images. The images contained records of artefact such as fossils but these did not exceed 0.1% of the total area. The binarization of the photographs taken from the slabs was one of the challenging aspects of this research and similar efforts performed in connection with the study of permeability of the limestone were given in Selvadurai (2019a, b). First, all the photographs were taken with the same light intensity, background, and camera to have a consistent photographic basis. In this research program, three different approaches were employed to binarize the photographs: (i) Separation of the black and white regions manually by analyzing the photographs; (ii) Analyzing the photographs completely using the MATLAB code; and (iii) Using a combination of these two approaches, which is the basis for the binarization presented here. While it seems more consistent and accurate to use the approach (ii), the procedure will not necessarily result in a more accurate result, since the integrity of black and white regions is not preserved in this method. Also, since these regions will be imported into the finite element modeling software and remodeled, the regions need to be simplified in this step, which decreases the accuracy. Therefore, it was finally decided to analyze the photos using MATLAB and then remove the heterogeneities manually using CorelDRAW™. The threshold value was selected such that the volume and area fractions estimated during the previous research studies (Selvadurai, 2017, 2019a, b) were preserved.

The black and white separations of the slab faces are more of a qualitative classification rather than a distinct quantitative separation, and the photographic images contain transition regions rather than definite black/white regions. An approach that accounted for transition regions (three or more separate regions) proved to be unfeasible. The final decision concerning the binarized regions was considered to be the most pragmatic way in which the

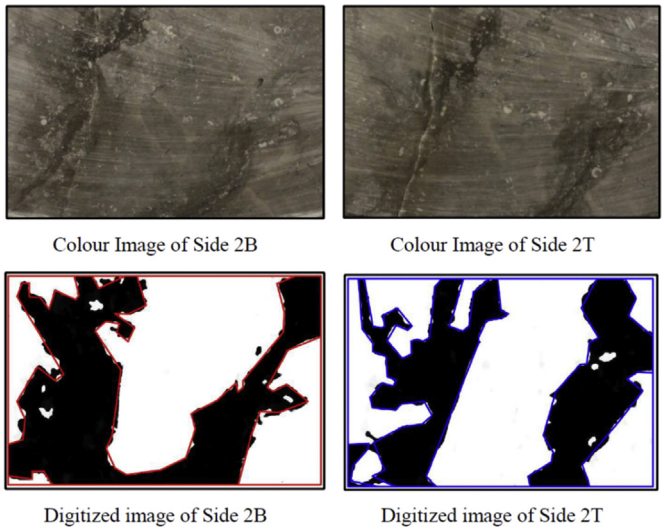

Fig. 3. Photographic and digitized images of the thick slab Section 2.

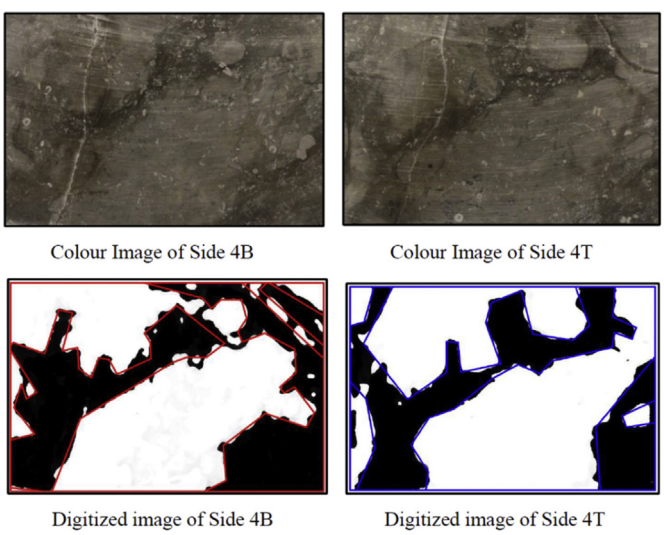

Fig. 4. Photographic and digitized images of the thick slab Section 4.

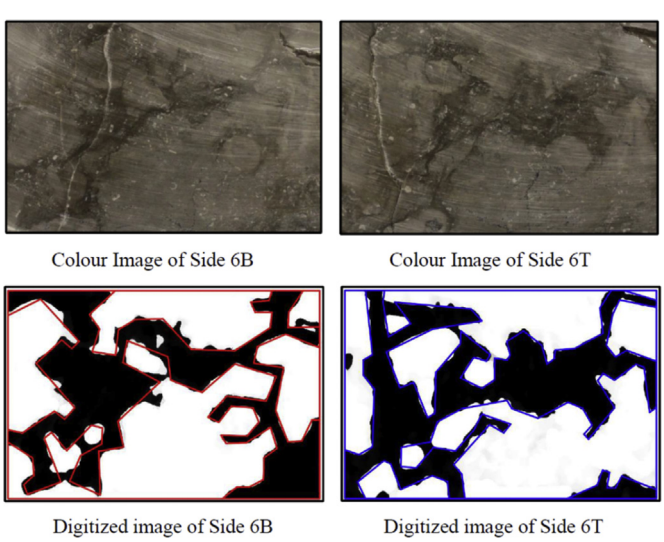

Fig. 5. Photographic and digitized images of the thick slab Section 6.

lighter and darker zones, defined according to the mineralogical compositions, could be delineated.

The black and white images were created using the CorelDRAW™ Graphics Suite X4. Typical examples are shown in Figs. 3–6. In these figures, the designation B and T refer, respectively, to the lower and upper surfaces of a thin slab. These images were used to reconstruct plausible replicas of the lighter and darker facies within the 8 mm thickness of each slab. In order to obtain through-thickness replicas of the internal facies distributions of the Cobourg limestone slabs, we adopted simple techniques that allow extrapolation of the surface images of the slabs to their interiors.

Here we adopted two simple techniques to create plausible distributions of the facies within each slab. Attention will be focused on the generation of the darker regions with the understanding that, in view of the very low porosity of both facies, the remaining regions correspond to the lighter domains. The simplest approach is to '*extrude*' the darker regions from either face to the mid-plane of the 8 mm thick slab. The second approach involves a solid modeling-type procedure that makes use of the LOFT command available in the software AutoCAD. The details of the reconstruction procedure were given by Selvadurai (2019b). For convenience of description, the geometry created using the LOFT command is referred to as the *Morphed* geometry. Figs. 7–10 show the typical replicas of the internal distribution of the lighter and darker facies in the thick slab specimen sections 2, 4, 6 and 8. Kriging techniques are an alternative procedure for estimating the internal distribution of properties using data available on the boundaries or surfaces of the domain (Selvadurai and Selvadurai, 2010, 2014). This approach has merit when the thicknesses of the slabs are large in comparison to the dimensions of the internal fabric.

The internal geometry of the facies within each thick slab of the Cobourg limestone is discretized as tetrahedral finite elements to create a three-dimensional (3D) replica of the thick slab that can then be used to model the heat conduction process. The effective thermal conductivities within each thick slab along *three orthogonal directions* can be determined by subjecting two opposite faces of the thick slab to constant temperatures (i.e. Dirichlet boundary conditions with constant values over each face but with a temperature differential between the two faces) and ensuring that the remaining adjacent faces are completely insulated (i.e. null Neumann boundary conditions). The effective thermal conductivities of the lighter and darker facies evaluated at 273 K and 373 K

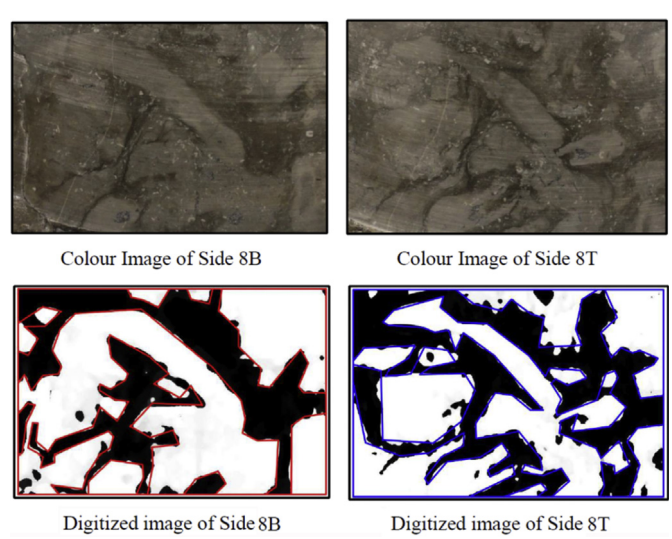

Fig. 6. Photographic and digitized images of the thick slab Section 8.

determined from the Hill (1952) estimates are used in the computational modeling, i.e. Eqs. (5) and (10).

The computational procedure can be applied to determine the effective thermal conductivities of each slab in three orthogonal directions. The computational model of each slab uses in excess of 210,000 elements and 280,000 degrees of freedom. It should be noted that by invoking null Neumann boundary conditions, the heat flow between slabs is suppressed. This is a limitation in the modeling approach; the alternative requires complete 3D modeling of all 10 assembled slabs with the appropriate boundary conditions to ensure one-dimensional heat flow through the assembly. This approach is computing intensive and was not pursued. The computational results derived from the modeling are summarized in Tables 4 and 5. For reference, the effective thermal conductivity of a slab normal to the plane area of the slab is denoted by k_z and the effective thermal conductivities for the directions aligned with the edges of the thick slab perpendicular to the z-direction are denoted by k_x and k_y.

The accuracy of the results presented in this study is controlled by the accuracy of the method employed and the accuracy level of the transport estimation in the lighter and darker regions. While the Hill (1952) estimate is used here to determine the thermal conductivity of lighter and darker regions, more accurate analysis can be performed by employing a range for the thermal conductivity of darker and lighter regions and determining the conductivity range of the overall sample.

To analyze the accuracy of the method, we performed another analysis, which is presented here. First, it should be mentioned that modeling the entire geometry resulting from combining all the slabs is not possible due to limitations of the finite element modeling software employed in this research. Multiple efforts to combine the geometries and mesh the overall geometry were unsuccessful due to limitations of the software. However, it was possible to combine four extruded slabs (slabs 7–10) and model the combined geometry; the results were compared with the weighted harmonic mean for k_z, and the weighted mean for in-plane conductivity in x- and y-direction, k_x and k_y, obtained from the data for the individual slabs. Considering the data for the temperature of 273 K, (i) the combined finite element model geometry gives $k_z = k_x = k_y = 3.793$ W/(m K), and (ii) the weighted mean and weighted harmonic mean estimates give $k_z = k_x = k_y = 3.793$ W/(m K). While this exact matching of quantities might be a coincidence, it suggests that the procedure for averaging the conductivities of the slabs to estimate the overall conductivity gives reasonably accurate estimates.

The results obtained from the finite element computations performed on the 10 thick slabs using the steady heat conduction analyses can now be combined to obtain the effective thermal conductivities for the assemblage. The weighted harmonic mean is used to estimate the effective thermal conductivity of the assembled cuboid of the Cobourg limestone in the direction normal to the plane of the plates and corresponds to $(k_z^*)_{273}^{\text{Extr}}$, $(k_z^*)_{273}^{\text{Morph}}$, $(k_z^*)_{373}^{\text{Extr}}$ and $(k_z^*)_{373}^{\text{Morph}}$. For the *extruded* geometry, we have

$$\left.\begin{aligned}(k_z^*)_{273}^{\text{Extr}} &= \frac{\sum_{i=1}^{10} t_i}{\sum_{i=1}^{10}\left[\dfrac{t_i}{\left(k_z^i\right)_{273}^{\text{Extr}}}\right]} \simeq 3.792 \text{ W/(m K)}\\ (k_z^*)_{273}^{\text{Morph}} &= \frac{\sum_{i=1}^{10} t_i}{\sum_{i=1}^{10}\left[\dfrac{t_i}{\left(k_z^i\right)_{273}^{\text{Morph}}}\right]} \simeq 3.791 \text{ W/(m K)}\end{aligned}\right\} \tag{12}$$

where t_i is the plate thickness; and $(k_z^i)_{273}^{\text{Extr}}$ and $(k_z^i)_{273}^{\text{Morph}}$ are the effective thermal conductivities of the Cobourg limestone slabs in direction normal to the plane of each slab for the extruded and

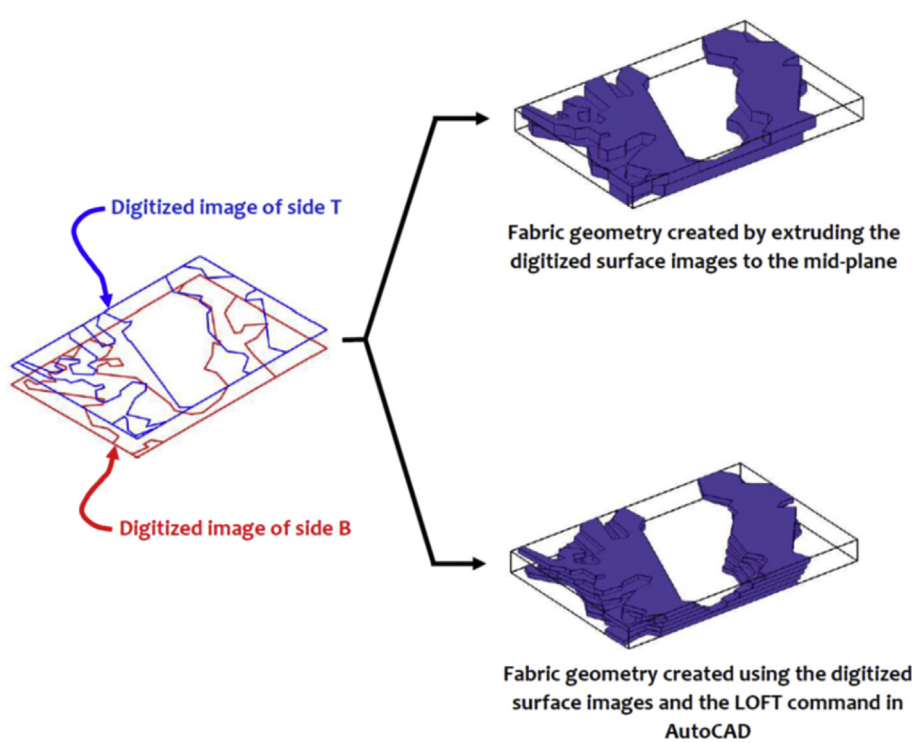

Fig. 7. Reconstructed domains identified for the finite element modeling of thick slab Section 2.

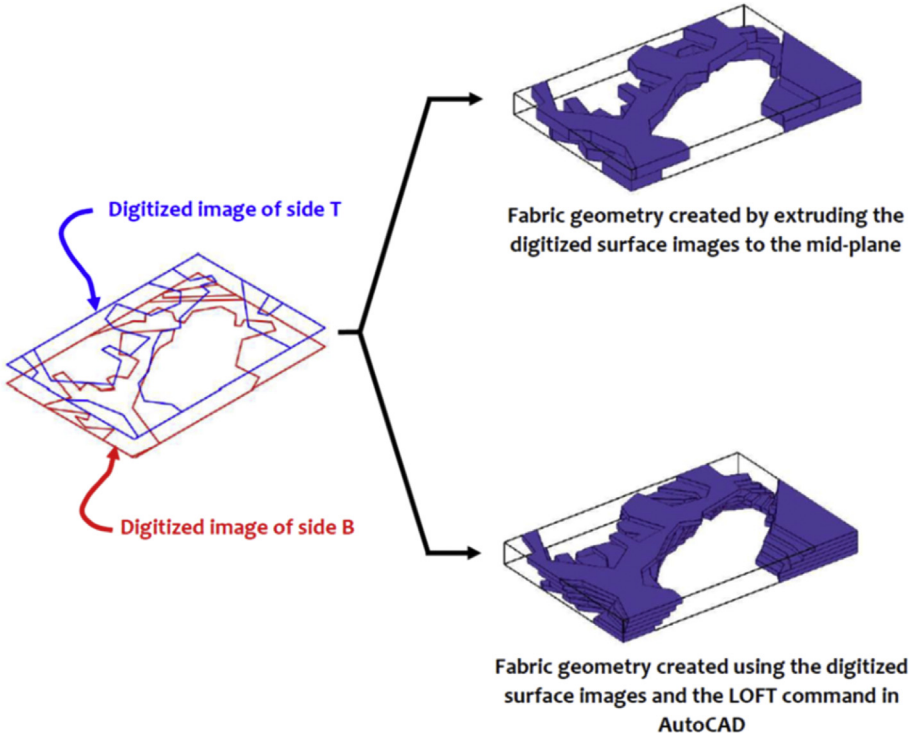

Fig. 8. Reconstructed domains identified for the finite element modeling of thick slab Section 4.

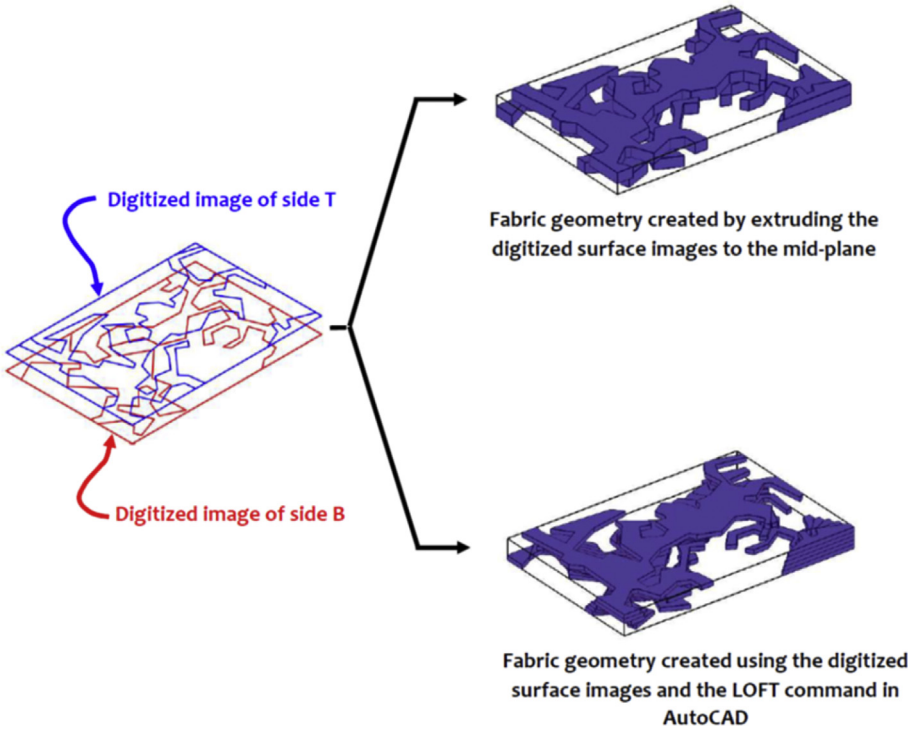

Fig. 9. Reconstructed domains identified for the finite element modeling of thick slab Section 6.

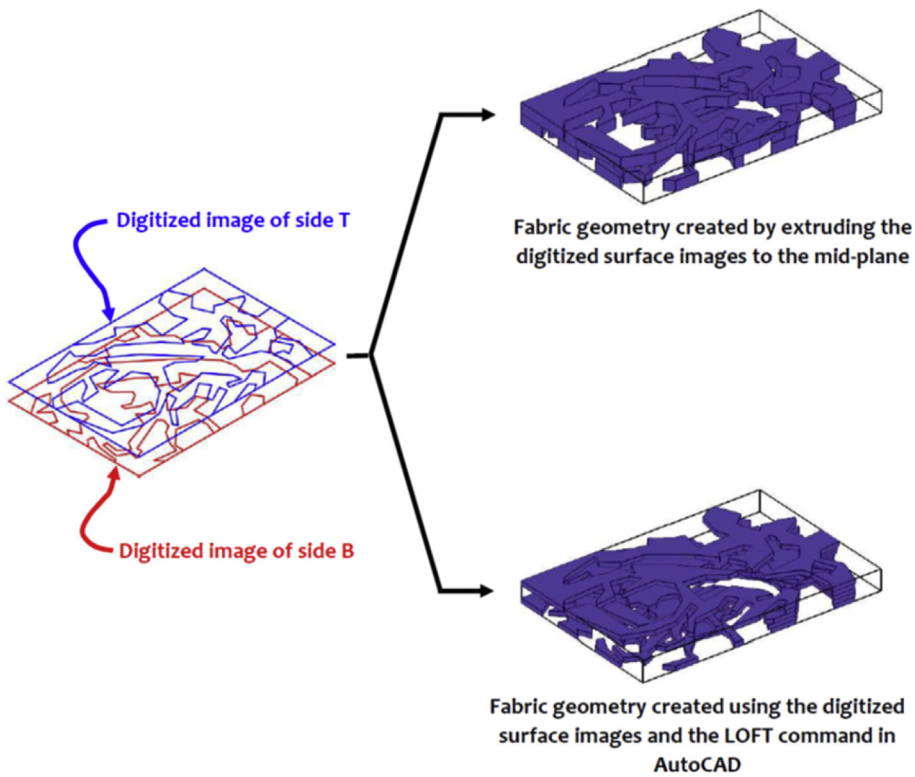

Fig. 10. Reconstructed domains identified for the finite element modeling of thick slab Section 8.

Table 4
Thermal conductivities of the individual slabs of the Cobourg limestone at 273 K derived from the COMSOL modeling ($(k^*_{273\ \mathrm{K}})_{\mathrm{LR}}$ = 3.78 W/(m K) and $(k^*_{273\ \mathrm{K}})_{\mathrm{DR}}$ = 3.81 W/(m K)).

Plate (i)	Thermal conductivity (W/(m K))					
	Extruded geometry			Morphed geometry		
	k^i_z	k^i_x	k^i_y	k^i_z	k^i_x	k^i_y
1	3.791	3.791	3.791	3.791	3.791	3.791
2	3.793	3.793	3.793	3.793	3.793	3.793
3	3.792	3.792	3.792	3.792	3.792	3.792
4	3.791	3.791	3.791	3.791	3.791	3.791
5	3.791	3.791	3.791	3.79	3.789	3.789
6	3.791	3.791	3.791	3.791	3.791	3.791
7	3.791	3.791	3.791	3.790	3.79	3.79
8	3.792	3.792	3.792	3.791	3.791	3.791
9	3.794	3.794	3.794	3.791	3.791	3.791
10	3.795	3.795	3.795	3.794	3.794	3.794

Table 5
Thermal conductivities of the individual slabs of the Cobourg limestone at 373 K derived from the COMSOL modeling ($(k^*_{373\ \mathrm{K}})_{\mathrm{LR}}$ = 2.94 W/(m K) and $(k^*_{373\ \mathrm{K}})_{\mathrm{DR}}$ = 2.98 W/(m K)).

Plate (i)	Thermal conductivity (W/(m K))					
	Extruded geometry			Morphed geometry		
	k^i_z	k^i_x	k^i_y	k^i_z	k^i_x	k^i_y
1	2.955	2.955	2.955	2.955	2.955	2.955
2	2.957	2.957	2.957	2.957	2.957	2.957
3	2.956	2.956	2.956	2.956	2.956	2.956
4	2.955	2.955	2.955	2.955	2.955	2.955
5	2.955	2.955	2.955	2.953	2.953	2.953
6	2.955	2.955	2.955	2.954	2.954	2.954
7	2.955	2.955	2.955	2.954	2.954	2.954
8	2.956	2.956	2.955	2.955	2.955	2.955
9	2.959	2.959	2.958	2.955	2.955	2.955
10	2.96	2.96	2.96	2.959	2.959	2.959

morphed geometries, respectively. Similarly, the weighted mean can be used to estimate the effective thermal conductivity of the assembled cuboid in directions orthogonal to the z-axis, denoted by x and y:

$$\left.\begin{aligned}(k^*_x)^{\mathrm{Extr}}_{273} &= \frac{\sum_{i=1}^{10}\left[\left(k^i_x\right)^{\mathrm{Extr}}_{273} t_i\right]}{\sum_{i=1}^{10} t_i} \simeq 3.792\ \mathrm{W/(m\ K)}\\ (k^*_x)^{\mathrm{Morph}}_{273} &= \frac{\sum_{i=1}^{10}\left[\left(k^i_x\right)^{\mathrm{Morph}}_{273} t_i\right]}{\sum_{i=1}^{10} t_i} \simeq 3.791\ \mathrm{W/(m\ K)}\end{aligned}\right\} \tag{13}$$

$$\left.\begin{aligned}\left(k^*_y\right)^{\mathrm{Extr}}_{273} &= \frac{\sum_{i=1}^{10}\left[\left(k^i_y\right)^{\mathrm{Extr}}_{273} t_i\right]}{\sum_{i=1}^{10} t_i} \simeq 3.792\ \mathrm{W/(m\ K)}\\ \left(k^*_y\right)^{\mathrm{Morph}}_{273} &= \frac{\sum_{i=1}^{10}\left[\left(k^i_y\right)^{\mathrm{Morph}}_{273} t_i\right]}{\sum_{i=1}^{10} t_i} \simeq 3.791\ \mathrm{W/(m\ K)}\end{aligned}\right\} \tag{14}$$

The procedure can be repeated to determine the thermal conductivities applicable to 373 K. The results are as follows:

$$\left.\begin{aligned}&(k_z^*)_{373}^{\text{Extr}} \simeq 2.956\ \text{W/(m K)};\quad (k_z^*)_{373}^{\text{Morph}} \simeq 2.955\ \text{W/(m K)}\\&(k_x^*)_{373}^{\text{Extr}} \simeq 2.956\ \text{W/(m K)};\quad (k_x^*)_{373}^{\text{Morph}} \simeq 2.955\ \text{W/(m K)}\\&\left(k_y^*\right)_{373}^{\text{Extr}} \simeq 2.956\ \text{W/(m K)};\quad \left(k_y^*\right)_{373}^{\text{Morph}} \simeq 2.955\ \text{W/(m K)}\end{aligned}\right\} \tag{15}$$

The results given in Eqs. (12)–(15) can be used to obtain the geometric mean for the effective thermal conductivities applicable to the temperatures of 273 K and 373 K, for the extruded and morphed fabric generations, i.e.

$$\left.\begin{aligned}&(k_{\text{GM}})_{273}^{\text{Extr}} = \sqrt[3]{(k_x^*)_{273}^{\text{Extr}}\left(k_y^*\right)_{273}^{\text{Extr}}(k_z^*)_{273}^{\text{Extr}}} \simeq 3.792\ \text{W/(m K)}\\&(k_{\text{GM}})_{273}^{\text{Morph}} = \sqrt[3]{(k_x^*)_{273}^{\text{Morph}}\left(k_y^*\right)_{273}^{\text{Morph}}(k_z^*)_{273}^{\text{Morph}}} \simeq 3.791\ \text{W/(m K)}\end{aligned}\right\} \tag{16}$$

Similarly, the geometric mean estimates for the thermal conductivities applicable to the temperature of 373 K are given by

$$\left.\begin{aligned}&(k_{\text{GM}})_{373}^{\text{Extr}} = \sqrt[3]{(k_x^*)_{373}^{\text{Extr}}\left(k_y^*\right)_{373}^{\text{Extr}}(k_z^*)_{373}^{\text{Extr}}} \simeq 2.956\ \text{W/(m K)}\\&(k_{\text{GM}})_{373}^{\text{Morph}} = \sqrt[3]{(k_x^*)_{373}^{\text{Morph}}\left(k_y^*\right)_{373}^{\text{Morph}}(k_z^*)_{373}^{\text{Morph}}} \simeq 2.955\ \text{W/(m K)}\end{aligned}\right\} \tag{17}$$

Considering the range of theoretical estimates for the effective thermal conductivities of the Cobourg limestone, it is concluded that the range of values are bounded by upper and lower limits:

$$\left.\begin{aligned}&3.791\ \text{W/(m K)} < k_{273\ \text{K}}^* < 3.792\ \text{W/(m K)}\\&2.955\ \text{W/(m K)} < k_{373\ \text{K}}^* < 2.956\ \text{W/(m K)}\end{aligned}\right\} \tag{18}$$

Experimental evaluation of the thermal conductivity of Cobourg limestone is rare. Selvadurai and Najari (2017) used a value of thermal conductivity of $k \simeq 2.5$ W/(m K) in their investigation of a saturated Cobourg limestone cylinder during boundary heating up to 70 °C. The results of Pitts (2017) suggest $k_{25\ ^\circ\text{C}} \simeq (3.04 \pm 0.9)$ W/(m K) and $k_{100\ ^\circ\text{C}} \simeq (1.44 \pm 0.9)$ W/(m K); these results indicate that there is a trend in the reduction in the thermal conductivity with an increase in the test temperature but this is lower than the theoretical estimates presented in this study. It should also be noted that, although standard procedures are available for performing experiments to obtain the thermal conductivity of geologic materials, the details of the experimental procedures including contact thermal resistances at imperfect contacts and abnormally high temperature gradients (Selvadurai, 1990, 2002) can influence the interpretation of experimental data when estimating the bulk thermal conductivity.

6. Concluding remarks

The paper presents alternative theoretical and computational procedures that can be used to estimate the thermal conductivity of a heterogeneous rock. The estimation is based on the mineralogical composition of the rock, which can be obtained quite accurately using conventional XRD tests. The accuracy and reliability of the theoretical evaluations rest on the accuracy with which (i) the mineralogical compositions and (ii) the thermal conductivities of the individual minerals can be estimated. In the case of the Cobourg limestone, there are visible lighter and darker heterogeneities that are both calcite-rich but contain varying proportions of dolomite, quartz and the clay minerals (illite, kaolinite and montmorillonite). This heterogeneity can lead to varying theoretical estimates based on the conventional Voigt (1928) and Reuss (1929) bounds and the Hill (1952) average and estimates based on the theoretical developments proposed by Hashin and Shtrikman (1962). These studies are complemented by computational models that are derived from 3D reconstructions of the lighter and darker regions of the rock present in 10 thick slabs of the limestone, measuring 80 mm × 100 mm × 8 mm, obtained by dissection of a cuboidal sample. These approaches have allowed the development of suitable bounds for the bulk thermal conductivity of the Cobourg limestone.

The reliability of the estimates for the bulk thermal conductivity of the Cobourg limestone ultimately depends on the accuracy with which the thermal conductivities of the minerals in the limestone can be determined. The estimation of the thermal properties of the minerals is not a routine exercise and requires access to sophisticated experimental procedures. The published literature, however, contains a wealth of information on thermal conductivity estimates for the minerals and these values are used in the development of the theoretical and computational estimates. The theoretical estimates for the bulk thermal conductivity of the Cobourg limestone are higher than those reported in the geotechnical literature, indicating that experimental procedures can introduce thermal resistances that can influence the experimentally-determined values of thermal conductivity. It should also be mentioned that the procedure presented in the paper is a convenient methodology that will be suitable when large test specimens are needed to capture RVEs in the scale of the heterogeneity.

Declaration of Competing Interest

The authors wish to confirm that there are no known conflicts of interests associated with this publication and there has been no significant financial support for this work that could have influenced its outcome.

Acknowledgments

The research support was provided by the Nuclear Waste Management Organization (NWMO), Toronto, Ontario, Canada, a Discovery Research Grant by the Natural Sciences and Engineering Research Council of Canada, and The James McGill Research Chairs Program. The authors are grateful to the Staff at Geoscience Research and Development at NWMO for their valuable comments on the drafts of the manuscript. The authors are grateful to Professor Martin Mazurek of the Rock–Water Interaction (RWI) Group, Institute of Geological Sciences, University of Bern, Switzerland, for drawing attention to their data on the mineralogical composition of the Cobourg limestone. A number of research assistants, graduate students and post-doctoral researchers in the Environmental Geomechanics Research group under the direction of the first author have contributed to the research program dealing with the Cobourg limestone. Their contributions are gratefully acknowledged.

References

Alonso EE, Alcoverro J, Coste F, Malinsky L, Merrien-Soukatchoff V, Kadiri I, Nowak T, Shao H, Nguyen TS, Selvadurai APS, Armand G, Sobolik SR, Itamura M, Stone CM, Webb SW, Rejeb A, Tijani M, Maouche Z, Kobayashi A, Kurikami H, Ito A, Sugita Y, Chijimatsu M, Börgesson L, Hernelind J, Rutqvist J, Tsang CF, Jussila P. The FEBEX benchmark test: case definition and comparison of modelling approaches. International Journal of Rock Mechanics and Mining Sciences 2005;42:611–38.

Biot MA. General theory of three-dimensional consolidation. Journal of Applied Physics 1941;12:155–64.
Birch AF, Clarke H. Thermal conductivity of rocks and its dependence upon temperature and composition, part 1. American Journal of Science 1940a;238:529–58.
Birch AF, Clarke H. Thermal conductivity of rocks and its dependence upon temperature and composition, part 2. American Journal of Science 1940b;238:613–35.
Brady PV, Arnold BW, Freeze GA, Swift PN, Bauer SJ, Kanney JL, Rechard RP, Stein JS. Deep borehole disposal of high-level radioactive waste. Technical Report SAND2009-4401. Albuquerque, NM, USA: Sandia National Laboratory; 2009.
Brigaud F, Vasseur G. Mineralogy, porosity and fluid control on thermal conductivity of sedimentary rocks. Geophysical Journal 1989;98:525–42.
Budiansky B. Thermal and thermoelastic properties of isotropic composites. Journal of Composite Materials 1970;4:286–95.
Cermak V, Rybach L. Thermal properties: thermal conductivity and specific heat of minerals and rocks. In: Landolt-Berenstein Zahlenwerte und Functionen aus Naturwissenschaften und Technik, Neue Serie, Physikalische Eigenschaften der Gesteine. Springer; 1982. p. 305–43.
Chapman NA, McKinley IG. The geological disposal of nuclear waste. Wiley; 1987.
Christensen RM. Mechanics of composite materials. Wiley-Interscience; 1979.
Côme B, Johnston P, Müller A, editors. Design and instrumentation of in situ experiments in underground laboratories for radioactive waste disposal: proceedings of the workshop jointly organized by commission of the European community and OECD nuclear energy agency. Brussels: A.A. Balkema; 1985.
Faybishenko B, Birkholzer J, Sassani D, Swift P, editors. International approaches for deep geological disposal of nuclear waste: geological challenges in radioactive waste isolation - fifth worldwide review. Lawrence Berkeley National Laboratory; 2016. LBNL-1006984.
Fourier JB. Théorie analytique de la chaleur, Chez Firmin Didot. Paris, France: Pére et Fils; 1822 (in Germany).
Gnirk P. OECD/NEA international stripa project, overview volume II: natural barriers, Sweden. Stockholm, Sweden; SKB. 1993.
Gray MN. OECD/NEA international stripa project, overview volume III: engineered barriers, Sweden. Stockholm, Sweden; SKB. 1993.
Hashin Z, Shtrikman S. A variational approach to the theory of effective magnetic permeability of multi-phase materials. Journal of Applied Physics 1962;33:3125–31.
Hill R. The elastic behaviour of a crystalline aggregate. Proceedings of the Physical Society A 1952;65:349–54.
Horai K. Thermal conductivity of rock-forming minerals. Journal of Geophysical Research 1971;76:1278–308.
Horai K, Simmons G. Thermal conductivity of rock-forming minerals. Earth and Planetary Science Letters 1969;6:359–68.
IAEA. Scientific and technical basis for geologic disposal of radioactive waste. Technical Reports Series No. 413. Vienna, Austria: International Atomic Energy Agency (IAEA); 2000.
Kappelmeyer O, Haenel R. Geothermics with special reference to applications. In: Berlin gebrueder borntraeger geoexploration monographs series; 1974.
Koroleva M, de Haller A, Mäder U, Niklaus H, Mazurek M. Borehole DGR-2: porewater investigations. Technical report TR 08-02. Bern. Switzerland: Rock-Water Interaction (RWI), Institute of Geological Sciences, University of Bern; 2009.
Laughton AS, Roberts LEJ, Wilkinson D, Gray DA. The disposal of long-lived and highly radioactive wastes. In: Proceedings of a royal society discussion meeting. London, UK: Royal Society; 1986.
Merriman JD, Hofmeister AM, Roy DJ, Whittington AG. Temperature-dependent thermal properties of carbonate minerals and rocks. Geosphere 2018;14:1961–87.
NIREX. A review of the deep borehole disposal concept for radioactive waste. Technical Report No. N/108. United Kingdom Nirex Limited; 2004.
NWMO. Ontario Power Generation's deep geologic repository for low and intermediate level waste: post Closure Safety Assessment. Technical Report NWMO DGR-TR-2011-25. Nuclear Waste Management Organization (NWMO); 2011a.
NWMO. Ontario Power Generation's deep geologic repository for low and intermediate level waste: geosynthesis. Technical Report NWMO DGR-TR-2011-11. Nuclear Waste Management Organization (NWMO); 2011b.
OECD. Geological disposal of radioactive waste: in situ research and investigation in OECD countries. Paris, France: Nuclear Energy Agency (NEA) Advisory Group, organization for Economic Cooperation and Development (OECD); 1988.
OPG. Ontario Power Generation's deep geologic repository for low and intermediate level waste: DGR: protecting Lake Huron. Ontario Power Generation. 2016. http://www.opg.com/dgr.
Pitts M. Thermal properties of the Cobourg limestone. MSc Thesis. Kingston, ON, Canada: Queen's University; 2017.
Pribnow D, Umsonst T. Estimation of thermal conductivity from the mineral composition: influence of fabric and anisotropy. Geophysical Research Letters 1993;20:2199–202.
Pusch R, Yong RN, Nakano M. High-level radioactive waste (HLW) disposal: a global challenge. Southampton, UK: WIT Press; 2011.
Reuss A. Berechnung der Fließgrenze von Mischkristallen auf Grund der Plastizitätsbedingung für Einkristalle. Journal of Applied Mathematics and Mechanics 1929;9:49–58 (in German).
Revil A. Thermal conductivity of unconsolidated sediments with geophysical applications. Journal of Geophysical Research 2000;105:16749–68.
Robertson EC. Thermal properties of rocks. Geological survey report, vols. 88–441. Reston Virginia, USA: Department of the Interior; 1988.
Rutqvist J, Rejeb AMT, Tsang CF. Analyses of coupled hydrological-mechanical effects during drilling of the FEBEX tunnel at Grimsel. In: Elsevier Geo-Engineering Book Series, 2; 2004. p. 131–6.
Rutqvist J, Chijimatsu M, Jing L, de Jonge J, Kohlmeier M, Millard A, Nguyen TS, Rejeb A, Souley M, Sugita Y, Tsang CF. Numerical study of the THM effects on the near-field safety of a hypothetical nuclear waste repository—BMT1 of the DECOVALEX III project. Part 3: effects of THM coupling in fractured rock. International Journal of Rock Mechanics and Mining Sciences 2005;42:745–55.
Selvadurai APS. Heat-induced moisture movement within a clay-based sealing material. Engineering Geology 1990;28(1–4):325–35.
Selvadurai APS, editor. Hydro-thermo-mechanics of engineered clay barriers and geological barriers. Special Issue Engineering Geology, vol. 47; 1997. p. 311–79.
Selvadurai APS. Influence of pressurized water influx on the hydro-thermal behaviour of an engineered clay barrier in a waste emplacement borehole. Engineering Geology 2002;64:157–78.
Selvadurai APS. Geomechanical characterization of the Cobourg limestone. Nuclear Waste Management Organization (NWMO); 2017. Technical Report NWMO-TR-2017-7.
Selvadurai APS. The Biot coefficient for a low permeability heterogeneous limestone. Continuum Mechanics and Thermodynamics 2019a;31:939–53.
Selvadurai APS. A multi-phasic perspective of the intact permeability of the heterogeneous argillaceous Cobourg limestone. Scientific Reports 2019b;9:17388. https://doi.org/10.1038/s41598-019-53343-7.
Selvadurai APS, Głowacki A. Stress-induced permeability alterations in an argillaceous limestone. Rock Mechanics and Rock Engineering 2017;50(5):1079–96.
Selvadurai APS, Głowacki A. Estimates for the local permeability of the Cobourg limestone. Journal of Rock Mechanics and Geotechnical Engineering 2018;10(6):1009–19.
Selvadurai APS, Jenner L. Radial flow permeability testing of an argillaceous limestone. Ground Water 2013;51(1):100–7.
Selvadurai APS, Najari M. Isothermal permeability of the argillaceous Cobourg limestone. Oil and Gas Science and Technology 2016;71(4):53. https://doi.org/10.2516/ogst/2015039.
Selvadurai APS, Najari M. The thermo-hydro-mechanical behavior of the argillaceous Cobourg Limestone. Journal of Geophysical Research: Solid Earth 2017;122:4157–71.
Selvadurai APS, Nguyen TS. Computational modelling of isothermal consolidation of fractured porous media. Computers and Geotechnics 1995;17(1):39–73.
Selvadurai APS, Nguyen TS. Scoping analyses of the coupled thermal-hydrological-mechanical behaviour of the rock mass around a nuclear fuel waste repository. Engineering Geology 1996;47(4):379–400.
Selvadurai APS, Selvadurai PA. Surface permeability test: experiments and modeling for estimating effective permeability. Proceedings of the Royal Society Series A: Mathematical and Physical Sciences 2010;466:2819–46.
Selvadurai PA, Selvadurai APS. On the effective permeability of a heterogeneous porous medium: the role of the geometric mean. Philosophical Magazine 2014;94(20):2318–38.
Selvadurai APS, Suvorov AP. Thermo-poroelasticity and geomechanics. Cambridge, UK: Cambridge University Press; 2016.
Selvadurai APS, Letendre A, Hekimi B. Axial flow hydraulic pulse testing of an argillaceous limestone. Environmental Earth Science 2011;64:2047–58.
Selvadurai APS, Suvorov AP, Selvadurai PA. Thermo-hydro-mechanical processes in fractured rock formations during a glacial advance. Geoscientific Model Development 2015;8:2167–85.
Selvadurai APS, Selvadurai PA, Nejati M. A multi-phasic approach for estimating the Biot coefficient for Grimsel granite. Solid Earth 2019;10:2001–14.
Stephansson O, Jing L, Tsang CF, editors. Coupled thermo-hydro-mechanical processes of fractured media. Developments in Geotechnical Engineering, vol. 79. Amsterdam, the Netherlands: Elsevier Scientific Publications; 1996.
Vasseur G, Brigaud F, Demongodin L. Thermal conductivity estimation in sedimentary basins. Tectonophysics 1995;244:167–74.
Vilks P, Miller NH. Evaluation of experimental protocols for characterizing diffusion in sedimentary rocks. Nuclear Waste Management Division Report TR-2007-11. Toronto, Ontario, Canada: Atomic Energy of Canada Limited; 2007.
Voigt W. Lehrbuch der Kristallphysik. Leipzig, Germany: B.G. Teubner; 1928 (in German).
Waber HN, Mäder UK, Koroleva M, de Haller A. Testing methods for the characterization of saline pore water in an Ordovician limestone (Cobourg formation, St Mary's Quarry, Ontario) feasibility study. Switzerland: Rock-Water Interaction (RWI), Institute of Geological Sciences, University of Bern; 2007. Technical Report TR 07-01. Bern.
Wiener O. Die Theorie des Mischkörpers für das Feld des stationaären Strömung. Erste Abhandlung die Mittelswertesätsze für Kraft, Polarisation und. Energie. . Abh. Math.-Physischen Klasse Königl. Sächs Gesell. Wissen 1912;32:509–604 (in German).
Yardley BWD, Ewing RC, Whittleston RA. Deep-mined geological disposal of radioactive waste. Elements 2016;12:233–74.

Professor A.P.S. Selvadurai is William Scott Professor and Distinguished James McGill Professor in the Department of Civil Engineering and Applied Mechanics at McGill University. He received his PhD and DSc degrees in Theoretical Mechanics from the University of Nottingham. His research areas include nonlinear continuum mechanics and theoretical, computational and experimental geomechanics. He is the author or co-author of several research articles in these topics (http://www.mcgill.ca/civil/people/selvadurai/list-research-publications) and has either authored or co-authored texts on soil-structure interaction, elasticity and geomechanics, plasticity and geomechanics, partial differential equations in mechanics, transport phenomena in porous media and thermo-poroelasticity and geomechanics. He serves on the Editorial Boards of eleven leading Journals devoted to mechanics, geomechanics and engineering mathematics. He is a fellow of several societies including the Royal Society of Canada, The American Academy of Mechanics, The Institute of Mathematics and its Applications and the Canadian Academy of Engineering.

Dr. S.M. Rezaei Niya is a Research Fellow at RMIT University in Melbourne, Australia. He is conducting research on energy storage funded by the Australian Renewable Energy Agency (ARENA). Following completion of his PhD in Mechanical Engineering on transport characteristics of fuel cells at the University of British Columbia, he was awarded a Postdoctoral Fellowship by the National Sciences and Engineering Research Council of Canada (NSERC-PDF). Dr. Niya's research in transport analysis in porous structures initiated from his expertise obtained during his Postdoctoral Fellowship at Stanford University and Research Associateship at McGill University where he developed a novel modeling approach for examining transport processes in porous media.